Published in final edited form as:

Annu Rev Anal Chem (Palo Alto Calif). 2017 June 12; 10(1): 71–92. doi:10.1146/annurev-anchem-061516-045212.

Coupling Front-End Separations, Ion Mobility Spectrometry, and Mass Spectrometry For Enhanced Multidimensional Biological and Environmental Analyses

Xueyun Zheng[1], **Roza Wojcik**[1], **Xing Zhang**[2], **Yehia M. Ibrahim**[1], **Kristin E. Burnum-Johnson**[1], **Daniel J. Orton**[1], **Matthew E. Monroe**[1], **Ronald J. Moore**[1], **Richard D. Smith**[1], and **Erin S. Baker**[1]

[1]Earth and Biological Sciences Directorate, Pacific Northwest National Laboratory, Richland, Washington 99352

[2]Skaggs School of Pharmacy and Pharmaceutical Sciences, Anschutz Medical Campus, University of Colorado, Denver, Colorado 80045

Abstract

Ion mobility spectrometry (IMS) is a widely used analytical technique for rapid molecular separations in the gas phase. Though IMS alone is useful, its coupling with mass spectrometry (MS) and front-end separations is extremely beneficial for increasing measurement sensitivity, peak capacity of complex mixtures, and the scope of molecular information available from biological and environmental sample analyses. In fact, multiple disease screening and environmental evaluations have illustrated that the IMS-based multidimensional separations extract information that cannot be acquired with each technique individually. This review highlights three-dimensional separations using IMS-MS in conjunction with a range of front-end techniques, such as gas chromatography, supercritical fluid chromatography, liquid chromatography, solid-phase extractions, capillary electrophoresis, field asymmetric ion mobility spectrometry, and microfluidic devices. The origination, current state, various applications, and future capabilities of these multidimensional approaches are described in detail to provide insight into their uses and benefits.

Keywords

drift tube IMS; gas chromatography; supercritical fluid chromatography; liquid chromatography; solid-phase extraction; capillary electrophoresis; field asymmetric ion mobility spectrometry; microfluidics; structure for lossless ion manipulations

INTRODUCTION

The use of ion mobility spectrometry (IMS) in analytical measurements has skyrocketed over the last decade, with applications ranging from national security analyses, patient

DISCLOSURE STATEMENT

The authors are not aware of any affiliations, memberships, funding, or financial holdings that might be perceived as affecting the objectivity of this review.

screening, and environmental monitoring (1–8). IMS separates ions based on the balance of two forces that impact the ion movement, namely, the electric field pulling force and the frictional drag force due to collisions with the buffer gas molecules (9, 10). Different ways of applying the electric field and stationary state of the buffer gas have given rise to multiple IMS-based platforms, such as drift tube IMS (DTIMS) (11–14), traveling wave IMS (TWIMS) (15), trapped IMS (TIMS) (16), overtone IMS (OIMS) (17, 18), differential IMS (DIMS) (19), field asymmetric IMS (FAIMS) (20–22), and transversal modulation IMS (TM-IMS) (23). Although each form has proven to be powerful for separating ions in diverse applications, this review mainly focuses on DTIMS and occasionally indicates where the other techniques have been applied.

Despite the fact that interest in DTIMS has greatly increased over the last decade, it is not a new analytical technique. In fact, its foundation and that of mass spectrometry (MS) can be traced back to the X-ray experiments of Thomson and Rutherford in the late 1800s (24, 25). In classical DTIMS, ions are pulled through a drift tube filled with gas using a weak electric field, and the ions collide with the stationary buffer gas molecules. These interactions cause compact ions with smaller collision cross sections to drift faster than extended ions with large collision cross sections (Figure 1). The charge of the ion also has an effect on its drift time because the electric field pulls ions with more charges faster, allowing highly charged ions to travel faster than 1+ ions of the same molecular class. Because separate peaks are observed for each ion shape, DTIMS has several attractive features. First, it is able to resolve sequence and structural isomers that are indistinguishable in MS measurements (26–29). Second, peak congestion at the detector is reduced by distributing the ions on the basis of their shape and charge state differences. Third, structural identification of known and unknown molecules is possible by calculating each ion's experimental collision cross section (CCS) for comparison with molecular modeling calculations (28–30). Finally, the rapid DTIMS measurements are easily coupled with time-of-flight MS instruments for nested data acquisition of both shape and m/z information into a single DTIMS-MS experiment (31). This review outlines the basic method of injected-DTIMS-MS and then describes multidimensional approaches that have a front-end separation coupled to DTIMS-MS.

INJECTED-DRIFT TUBE ION MOBILITY SPECTROMETRY–MASS SPECTROMETRY

Currently, many DTIMS-MS measurements are performed by directly infusing or injecting the sample of interest into the IMS drift cell without a front-end separation. Injected-DTIMS-MS analyses are extensively used for the separation of many different types of molecules, with applications ranging from characterizing proteins to evaluating lipid extracts (32–35). Through significant technical developments during the late 1990s and early 2000s, higher-sensitivity DTIMS-MS instruments were created and made commercially available to the public (24). Two of the greatest challenges addressed for DTIMS in the last 10–20 years were its low-duty cycle and sensitivity. In DTIMS, the low-duty cycle occurred because ions are traditionally only pulsed into the drift cell after those from the previous packet exit so that only a small percentage of ions created in the source are utilized. To address this

constraint, a multiplexing approach based on the Hadamard transform was developed, allowing multiple discreet ion packets to coexist in the drift cell as long as they do not overlap due to diffusional broadening (36). This approach enabled a much higher DTIMS duty cycle, a significant increase in measurement sensitivity, and a dramatic reduction in spectra noise due to deconvolution of the pseudorandom sequence. Multiplexing thus provided a much higher signal-to-noise ratio for the resulting spectra and greatly increased measurement duty cycle (37).

The DTIMS low sensitivity challenge was partially due to the low-duty cycle addressed with multiplexing, but mainly originated at the source and MS interface designs. Because DTIMS can be performed at pressures ranging from a few torr to above atmospheric pressure, interface optimization is extremely important when coupling the drift tube to the source and mass spectrometer. In atmospheric DTIMS instruments, the source interface does not need as much consideration as low-pressure DTIMS instruments because the pressures are equivalent. However, in low-pressure DTIMS, the pressure differences in the atmospheric source and low-pressure drift tube can cause significant ion losses if not correctly constructed. Thus, both single and dual ion funnel designs have been implemented prior to the low pressure IMS drift tube to reduce the high source pressure and refocus the ions prior to DTIMS separation (38). The drift tube exit can also have huge losses because the ions diffuse as they separate and they must be transported to the MS, which operates at very low $\sim 10^{-7}$ torr pressures. Therefore, an ion funnel is also often used after the drift tube to refocus the diffused ions prior to their transport through multiple transfer regions that decrease the pressure and allow detection by MS. The sensitivity gains provided by ion funnels have shown that they are essential for coupling IMS drift tubes with many different types of sources and mass spectrometers to create essentially lossless DTIMS-MS instruments (14).

The use of multiplexing and ion funnels have greatly improved DTIMS sensitivity and duty cycle, enabling faster DTIMS-MS measurements that can be coupled with various front-end separation techniques to achieve even higher peak capacity (39). In fact, many different front-end separation techniques, such as gas chromatography (GC), supercritical fluid chromatography (SFC), liquid chromatography (LC), solid-phase extractions (SPE), capillary electrophoresis (CE), FAIMS, and microfluidic devices, have been coupled with DTIMS-MS to date (Figure 1). These diverse three-dimensional (3D) measurements provide the ability to gain more information from environmental and biological analyses, but each have limitations (Table 1). In this review, we present the current state of these 3D techniques, illustrate their use in various applications, and speculate on their future capabilities.

GAS CHROMATOGRAPHY–DRIFT TUBE ION MOBILITY SPECTROMETRY–MASS SPECTROMETRY

GC was one of the first separation techniques coupled to DTIMS (11) and has important characteristics, such as highly reproducible chromatography and the ability to analyze compounds not possible with LC. GC separations usually take minutes to hours and are used

to analyze volatile compounds that can be vaporized without decomposition. Although GC is similar to LC, it has two noticeable differences. First, the separation occurs between a stationary phase coating and a gas mobile phase, whereas in LC the stationary phase is a solid and the mobile phase is a liquid. Second, the GC column is located in an oven, whereas LC is normally performed at much cooler column temperatures. In the earliest coupling of DTIMS and GC, DTIMS was used as a detector for GC (11). These two-dimensional (2D) GC-DTIMS analyses proved to be more powerful than each technique alone due to the combination of the highly reproducible GC retention times and drift time information available for each ion as well as greater peak capacity. Furthermore, the GC separation allows ions to arrive separately to the ionizer for decreased charging effects (40). GC-DTIMS has been applied in the detection of explosive and volatile compounds in complex samples and for medical analyses (41–45). GC has also been coupled with other IMS techniques. For instance, GC-DMS was recently installed on the International Space Station for real-time analysis of samples and for spaceflight water quality monitoring (46). Separately, GC-FAIMS was used to detect volatile organic compounds (47).

In 1970, the first 3D GC-DTIMS-MS configuration was reported by Cohen & Karasek (11) for organic chemical analysis with numerous applications occurring since then. One recent application of interest was a novel GC-DTIMS-MS platform, illustrated by Crawford et al. (48), which used secondary electrospray ionization (SESI) to enable more detailed and comprehensive investigations of complex mixtures (Figure 2). In this study, the GC was connected to DTIMS-MS via a heated transfer line so gaseous analytes could be introduced into the reaction region of the IMS. These GC preseparated analytes were subsequently ionized by SESI, pulsed into the IMS drift region for mobility separation, and detected by MS. Figure 2b shows 3D data obtained from the GC-DTIMS-MS analysis of lavender oil. The highlighted peaks (in white boxes) illustrate the separation of analytes by GC only, DTIMS only, and both GC and DTIMS. This 3D technique illustrates the greater degree of separation for a complex mixture compared to one-dimensional (1D) and 2D analyses (48). With the growing interest in small-molecule studies for many applications, we believe that GC-DTIMS-MS analyses of biological and environmental samples will greatly increase in the coming years.

SUPERCRITICAL FLUID CHROMATOGRAPHY–DRIFT TUBE ION MOBILITY SPECTROMETRY–MASS SPECTROMETRY

SFC was invented by Klesper et al. in 1962 (49) to extend the capability of GC by supporting the analysis of heavier compounds that require high temperature for elution but risk thermal decomposition at these elevated temperatures. In SFC analyses, carbon dioxide is used as the principle mobile phase solvent and is mixed with other cosolvents such as methanol to form the gradient. Over the last few years, there has been a growing interest in pharmaceutical analysis with SFC and SFC-MS due to recent technological advancements making the SFC instruments more sensitive (50–52). DTIMS was first coupled with SFC in the 1980s by Hill and coworkers (53–56) and used as a detector for organic compounds. Unfortunately, SFC limitations, such as difficulties analyzing polar compounds and the inherent low sensitivity, reduced its utility. These same challenges have limited other

applications of SFC-DTIMS-MS, with only one other study reported to date. This study sought to characterize nonsteroidal-selective androgen receptor modulators and detect enobosarm in bovine urine; however, results were very promising and showed the utility of SFC-DTIMS-MS if the limitations could be addressed (57). Thus, SFC-DTIMS-MS analyses are expected to increase, especially because SFC can provide an orthogonal separation capability comparable to LC.

LIQUID CHROMATOGRAPHY–DRIFT TUBE ION MOBILITY SPECTROMETRY–MASS SPECTROMETRY

To date, LC is the technique most coupled with DTIMS-MS. Although LC separations require minute- to hour-long timescales, they also allow greater molecular separations and higher peak capacity measurements. The earliest use of LC dates back to 1855 when filter paper impregnated with chemicals was used to separate dyes and create unique color patterns due to differential adsorption. Modern LC separations are normally utilized to separate molecules by various physicochemical properties using different column packing materials and mobile phase buffers. In the early 1990s, poor electrospray ionization (ESI) stability discouraged efforts in the hyphenation of the LC solution phase separation with the gas-phase DTIMS and MS techniques. However, technology developments in the mid-1990s solved these ESI problems and enabled LC to be coupled with DTIMS, TWIMS, and FAIMS for the acquisition of 3D spectra with LC elution times, IMS drift times (or CCS values), and m/z ratios for all detected ions in a sample (Figure 3) (39, 58).

The power of LC-DTIMS-MS was first illustrated in 2001 by Clemmer and colleagues (60) for a proteomic study of tryptic peptides arising from the digestion of five proteins (bovine and pig albumin, horse cytochrome c, and dog and pig hemoglobin). The results from this and several other LC-DTIMS-MS proteomic studies have illustrated three main advantages over traditional LC-MS studies (39, 61, 62). First, the chemical noise interferences in congested spectra decrease due to the DTIMS separation, which allows for higher-sensitivity measurements and the detection of low-abundance ions even in the presence of species with much greater intensities (39, 61, 62). Second, long LC separation times can be reduced due to the multiple orthogonal separations, while still retaining the same or additional features as LC-MS (39). Finally, more information on each peptide feature is available for library matching due to the three dimensions resulting in fewer false positive hits (59). These advantages all point to the potential use of LC-DTIMS-MS in targeted and global omic applications. Consequently, LC-DTIMS-MS and LC-TWIMS-MS have been used to separate metabolites (63, 64), lipids (65, 66), proteins (67), peptides (39, 60, 62, 68–71), and glycans (72) in complex biological and environmental samples. Furthermore, to add even more peak capacity, 2D LC applications, such as those with strong cation exchange and reversed-phase gradients or high- and low-pH reverse-phase gradients, have been combined with DTIMS-MS for four-dimensional measurements and even better coverage of complex mixtures (73, 74). Overall, the multidimensional LC and 2D LC-DTIMS-MS platforms have greatly improved the analytical sensitivity and specificity of LC-MS analyses. In addition, they have enhanced the measurement dynamic range and provided reliable identification and quantitation of low-abundance analyte species in complex biological matrices. Although

these benefits are very exciting, analysis of the multidimensional data is challenging and limits the full utility of these measurements. However, the recent incorporation of IMS drift time and CCS information into bioinformatics tools such as Skyline (75) has shown great promise for deconvolving the data obtained from these complex multidimensional studies.

SOLID-PHASE EXTRACTION–DRIFT TUBE ION MOBILITY SPECTROMETRY–MASS SPECTROMETRY

Due to the long analysis times required for LC separations, recent automated SPE techniques are of great interest for low-peak capacity LC separations with much higher throughput. SPE is one of the most frequently employed procedures to clean up, extract, fractionate, and preconcentrate biological and environmental samples (76). SPE is also useful in desalting, derivatizing, and buffer exchanging samples. Recently, online and automated SPE techniques have become popular for high-throughput studies in which the analyte class of interest is retained on a specific column or cartridge, eluted with the appropriate solvents, and measured in the eluate (77, 78). The main attraction of online SPE is that it greatly reduces sample preparation time and enables automation of conditioning, washing, elution, and reequilibration, thus increasing sample throughput. Analyte losses by evaporation are also often eliminated, and the solvent consumption is much lower, reducing the risk of the exposure to infectious samples or toxic solvents. In addition, online SPE cartridges are often reusable for thousands of samples, greatly decreasing material costs (77, 78).

One specific high-throughput automated SPE system is the Rapidfire SPE platform, which was originally introduced by BIOCIUS Life Sciences, Inc. and later acquired by Agilent Technologies (Santa Clara, CA). Briefly, the Rapidfire SPE system contains specially designed equipment, including an autosampler, LC pumps, SPE cartridges, and switching valves for ultrafast online sample preparation in which 5–10 μL of sample is directly aspirated from 96- or 384-well assay plates and loaded onto the microscale SPE cartridge using specific buffers. The analytes of interest are retained in the cartridge while the salts and buffers are washed away. A valve is then switched to send the flow path to the mass spectrometer, and appropriate organic solvents are delivered to elute the compounds off the cartridges for MS analysis. Because the typical cycle time including loading, wash, elution, and reequilibration is normally 10 s or less, these analyses are two to three orders of magnitude faster than conventional GC or LC techniques. The SPE cartridges can also be packed with different materials, such as C4, C8, C18, graphitic carbon, cyano, phenyl, and HILIC, providing broad extraction for various analytes in complex environmental and biological samples, such as urine and plasma. To date, the Rapidfire SPE system has been applied in several MS studies for ultrafast and high-throughput biological, biomedical, and drug discovery studies (79–86). Recently, this SPE system was coupled with DTIMS, demonstrating the first high-throughput online SPE-DTIMS-MS platform for fast sampling and multidimensional separations (87). This method also allowed simultaneous targeted and global measurements for the detection of thousands of endogenous metabolites and xenobiotics in complex human biofluids in <1 min total analysis time even when several cartridge types were used (Figure 4). Overall, the SPE-DTIMS-MS platform provides an

appealing tool to quickly screen for disease-specific molecules and monitor environmental exposures in large sample sizes (87).

Miniaturization of SPE to improve sample preparation efficiency was also demonstrated with solid-phase microextraction (SPME). SPME is performed when a fiber is coated with a thin layer of sorbent material, integrating extraction, concentration, and sample introduction into a single step (88). SPME was used in combination with GC-, LC-, and CE-MS and applied in environmental analysis, food chemistry, and biological fluids (89–92). SPME-DTIMS was also applied in explosive detection, degradation of chemical warfare agents in the environment, drug analysis, and biological studies and shows great utility in future multidimensional analyses (93–97).

CAPILLARY ELECTROPHORESIS–DRIFT TUBE ION MOBILITY SPECTROMETRY–MASS SPECTROMETRY

CE shares several commonalities with IMS separations, and in Revercomb & Mason's 1975 review (98), DTIMS was even referred to as gaseous electrophoresis. Similar to DTIMS, the separation efficiency of free-solution electrophoresis or capillary zone electrophoresis (CZE) is proportional to the applied electric field and inversely proportional to the diffusion coefficient of the analytes. Specifically, in DTIMS, an ion's mobility depends on its charge and is inversely proportional to its reduced mass and CCS, whereas in CZE, an ion's mobility is proportional to the net charge of the ion and inversely proportional to its friction coefficient in solution, which is related to the mass, shape, and hydrodynamic radius of the ion in solution. Physical properties of the separation buffer, such as pH, viscosity, dielectric strength, ionic strength, and temperature also impact the separation efficiency and selectivity in CZE (99–102). Not surprisingly, DTIMS-MS and CE also share common applications and are recognized as orthogonal to LC (103). Despite these commonalities, only a few cases of CE and DTIMS-MS as complementary or comparative techniques exist (104, 105). The first attempt to couple CE and DTIMS was performed by the Hill group in 1989 (106) with their newly developed ESI source for the IMS instrument (107). However, spray instability made this coupling difficult and hindered its initial application. Also during that time, issues with CE operational robustness, electrical circuit closure, and sample dilution limited the sensitivity of CE and hampered its widespread use with MS. In 2004, a CE-FAIMS-MS analysis of lipopolysasscharides indicated the promise of coupling these technologies, with CE separating the ions, FAIMS reducing the background noise, and MS determining the species present. All three separations attained three orders of magnitude linear dynamic range and provided highly informative data for the sample (Figure 5) (108, 109).

One challenge with CE and DTIMS is that their orthogonality has not been carefully evaluated thus far. However, despite certain similarities in their separation mechanisms, the orthogonality can be manipulated by the choice of CE separation buffers, voltage polarity, capillary surface charge, stacking techniques, and sheath liquid compositions. With these options for increasing the orthogonality of CE and DTIMS and the multiple technical advances over the last decade addressing the constraints in coupling liquid phase separations

with DTIMS (110–114), one can expect an increase in online CE-DTIMS-MS technologies in the near future.

FIELD ASYMMETRIC–AND DRIFT TUBE ION MOBILITY SPECTROMETRY–MASS SPECTROMETRY

Although FAIMS is performed after ionization and cannot reduce ionization suppression, it is another high-throughput separation that shows potential for the rapid analysis of complex samples when coupled with DTIMS. FAIMS is a scanning technique that originated during the early 1980s as a portable tool for chemical detection (115). Over the past two decades, it has emerged as a powerful analytical device for noise reduction in complex samples and targeted analyses (116). In FAIMS, ions oscillate between two electrodes as they travel through the device, alternately experiencing asymmetric strong and weak electric fields. After a number of cycles of the asymmetric waveform, if the mobility of an ion is greater in one direction than in the other, the ion will be lost as it deflects and collides with the electrode. However, an ion can be transmitted through the FAIMS device when a compensation field (CF) is superimposed to offset the ion's trajectory, so for each measurement the CF is scanned to selectively transmit ions from each sample (22, 117).

FAIMS is significantly different from conventional DTIMS in many ways (116, 118). The main differences are that FAIMS is a scanning technique, and not all ions can be observed under the same conditions as in DTIMS. Furthermore, unlike DTIMS that utilizes a constant low electric field, FAIMS operates at a wide range of E/N values (ratio of the electric field strength to the gas number density). Whereas the separation in DTIMS is based on an ion's CCS-to-charge ratio, the separation in FAIMS results from the mobility difference of the analyte and buffer gas interactions in both strong and weak electric fields. FAIMS has been utilized for pharmaceutical analyses (119), separating charge states (120, 121), and recently, its power to distinguish isobars (122), isomers (123), isotopomers (124), and protein conformers (125) has been highlighted. Both DTIMS and FAIMS have shown great potential in enhancing biological analyses when coupled with MS platforms by reducing chemical noise and detecting low-abundance analytes in complex biological matrices (126). DTIMS and FAIMS are also appealing because they offer analysis speeds that exceed condensed-phase separations by two to three orders of magnitude for rapid proteomic (127–129), lipidomic (130, 131), and other molecular analyses (109, 132).

The high-throughput nature and orthogonality of FAIMS and DTIMS drove the hyphenation of these two gas-phase separation techniques, with the initial 3D FAIMS-DTIMS-MS peptide analyses demonstrating a peak capacity of ~500 (133). However, this platform lacked measurement sensitivity due to the filtering nature of FAIMS and ion losses at the interface. Technological advances in the sensitivity of the ultra-FAIMS (μFAIMS) by the Owlstone firm (134, 135) prompted an additional evaluation of FAIMS-DTIMS-MS for 3D analyses of a bovine serum albumin tryptic digest and the separation of isomeric compounds (136). Although μFAIMS greatly improved the sensitivity of measurements, especially when utilizing a helium/nitrogen gas mixture as shown in Figure 6, its small size offered limited resolving power. In general, these studies showed that although coupling FAIMS with

DTIMS-MS can be challenging because of the losses in sensitivity, it can truly be a high-throughput analytical platform that offers multidimensional biological separations. However, to increase its future utility in complex sample studies, rapidly scanning FAIMS devices with higher sensitivity and resolution are needed to analyze samples quickly, while also gaining more measurement peak capacity in this short analysis period.

MICROFLUIDICS-DRIFT TUBE ION MOBILITY SPECTROMETRY–MASS SPECTROMETRY

Another technique that has not been extensively coupled with DTIMS-MS but shows great future promise is microfluidics. Microfluidics, or lab-on-a-chip technology, is a multidisciplinary field spanning engineering, physics, chemistry, biology, and nanotechnology and is applied to design analytical systems for small sample sizes, molecular biology, and biomedical research (137). Miniaturized chip-based devices utilize very low volumes of reagents and provide the benefit of easier sample and fluid handling and better experimental control, as well as lower costs for reagents and samples. With these numerous advantages, microfluidics has achieved many successes in automation, high-throughput screening, and in vitro diagnosis (137, 138). Coupling microfluidic devices with MS has also greatly enabled applications requiring fast analysis times, higher sensitivity, and higher throughputs. Moreover, multiple functions can be integrated onto just one chip, such as sample extraction, enzymatic digestion, derivatization, and separation, greatly simplifying operation procedures in high-throughput MS analyses (139–141).

Although microfluidic devices have greatly improved MS applications, their coupling to DTIMS-MS has been limited to only a few applications in protein/ligand binding (142) and real-time cellular studies (143, 144). The McLean group (143, 144) was the first to couple a mul-titrap nanophysiometer (MTNP) microfluidic device to TWIMS-MS in 2010. MTNP is used as a miniature reactor to study the real-time response of small cellular amounts to drugs and other perturbations. In the study by the McLean group (143), the microfluidic-TWIMS-MS analyses were used to monitor real-time cellular response to paracrine signals, changes in metabolite levels, and the delivery of drugs and toxins. Results from the measurements illustrated the possibility of not only detecting small amounts of biomolecular material but also measuring the materials with a temporal resolution of <5 min (143). A more mature platform integrating the MTNP microfluidic device with an online dual-column SPE desalter and TWIMS-MS platform further showed its capability of detecting cellular responses to microenvironmental stimuli, highlighting the potential for metabolite discovery applications (Figure 7) (144). Even though the SPE desalting process decreased the concentration of the metabolites from the small populations of cells, making the detection of lower concentration species difficult (144), the measurements obtained by coupling microfluidic devices with IMS-MS were quite exciting. Thus, we feel that given the advanced developments currently occurring in microfluidic technologies, there is a great possibility for more microfluidic devices being combined with DTIMS-MS in the near future.

DRIFT TUBE ION MOBILITY SPECTROMETRY–MASS SPECTROMETRY FUTURE DIRECTIONS

In this review, we summarize several currently used 3D techniques coupling DTIMS-MS with front-end separations, such as GC, SFC, LC, SPE, CE, FAIMS, and microfluidic devices. Although the origin of many of these techniques dates back 20–30 years, new technological developments for each separation are providing higher sensitivity and higher throughput measurements and enabling better 3D biological and environmental analyses compared to the 1D and 2D methods. However, to further benefit these 3D analyses and even increase the utility of DTIMS and DTIMS-MS studies, one challenge that must be addressed is the low DTIMS separation power of current measurements.

Low DTIMS separation power is a key drawback of the technique, as it limits the ability to distinguish many structurally similar molecules. This challenge restricts the range of molecular coverage possible, and in many cases, initiates the use of additional separation techniques as reviewed here. Higher DTIMS resolution would improve analysis coverage, separate structurally similar isomers, and increase the overall dynamic range of DTIMS measurements. Because the DTIMS resolving power is proportional to the square root of the drift field and length (145), these parameters have been investigated extensively. However, until recently, increasing drift cell length resulted in either large ion losses, low sensitivity, or a very limited molecular coverage due to the narrow mobility range that could be studied (146). Kemper et al. (147) built a 2-m DTIMS that achieved a resolving power of >100 to address this challenge; however, more length was still needed to separate many structurally similar isomers. Increasing the drift tube length past 2 m unfortunately requires extremely high voltages and long chambers, making it impractical for many laboratory spaces. To address this challenge, Merenbloom et al. (146) constructed a cyclic multipass drift tube in 2009. One constraint limiting their design was that the measureable mobility range decreased with every cycle needed to achieve greater separation. More recently, a cyclic design was developed based on the use of TWIMS, avoiding the high voltages needed in DTIMS but still limited by the cyclic path length (148). A promising new approach using structures for lossless ion manipulations (SLIM) was recently implemented to enable long-path DTIMS and TWIMS separations followed by MS analyses (Figure 8) (149, 150). This approach allowed the construction of a 13-m serpentine TWIMS drift path that provided previously unachieved resolution for biomolecules and more effective ion utilization, and it significantly improved characterization of very small sample sizes (149). These results demonstrated the potential for high-resolution proteomic, lipidomic, glycomic, and metabolomic IMS measurements. Furthermore, SLIM IMS technology developments are being performed to implement longer path lengths for even better separations, build ion reaction chambers for enhanced molecular characterizations, and increase the mobility window of analysis in high-resolution studies by using ion compression (151). Moreover, even though the serpentine path results to date have used TWIMS, it is expected that future developments will also allow DTIMS serpentine paths even if the higher voltages make it more challenging.

The ongoing technology developments to improve DTIMS resolution, manipulability, sensitivity, and duty cycle will continue to increase its future utility. Moreover, the rapid nature of DTIMS and its ability to be readily coupled with many techniques makes 1D, 2D, and multidimensional DTIMS–based analyses of great interest for difficult biological and environmental studies. To date, there are many complex problems that need the extensive molecular coverage and rapid perturbation sampling possible with the fast and highly sensitive DTIMS measurements. Single-cell analyses and microbial community studies are two areas that demand enormous technological improvements and provide many opportunities for DTIMS studies describing the numerous molecules present in each sample and varying under specific conditions. Additional applications, such as understanding the molecular causes of disease, assessing the effects of chemical exposure, and providing answers to new environmental and biological problems, are also expected to utilize DTIMS analyses extensively over the next decade.

Acknowledgments

The authors would like to thank Nathan Johnson for assistance in preparing the figures. Portions of this research were supported by grants from the National Institute of Environmental Health Sciences of the NIH (R01 ES022190), National Institute of General Medical Sciences (P41 GM103493), and the Laboratory Directed Research and Development Program and Microbes in Transition (MinT) Initiative at Pacific Northwest National Laboratory (PNNL). This research utilized capabilities developed by the Pan-omics program [funded by the US Department of Energy (DOE) Office of Biological and Environmental Research Genome Sciences Program] and by the National Institute of Allergy and Infectious Diseases under grant U19 AI106772. This work was performed in the W.R. Wiley Environmental Molecular Sciences Laboratory (EMSL), a DOE national scientific user facility at the PNNL. PNNL is operated by Battelle for the DOE under contract DE-AC05-76RL0 1830.

LITERATURE CITED

1. Ewing RG, Atkinson DA, Eiceman GA, Ewing GJ. A critical review of ion mobility spectrometry for the detection of explosives and explosive related compounds. Talanta. 2001; 54(3):515–29. [PubMed: 18968275]
2. Borsdorf H, Eiceman GA. Ion mobility spectrometry: principles and applications. Appl Spectrosc Rev. 2006; 41(4):323–75.
3. Mäkinen MA, Anttalainen OA, Sillanpää MET. Ion mobility spectrometry and its applications in detection of chemical warfare agents. Anal Chem. 2010; 82(23):9594–600. [PubMed: 20979419]
4. Armenta S, Alcala M, Blanco M. A review of recent, unconventional applications of ion mobility spectrometry (IMS). Anal Chim Acta. 2011; 703(2):114–23. [PubMed: 21889625]
5. Lapthorn C, Pullen F, Chowdhry BZ. Ion mobility spectrometry-mass spectrometry (IMS-MS) of small molecules: separating and assigning structures to ions. Mass Spectrom Rev. 2013; 32(1):43–71. [PubMed: 22941854]
6. Lanucara F, Holman SW, Gray CJ, Eyers CE. The power of ion mobility-mass spectrometry for structural characterization and the study of conformational dynamics. Nat Chem. 2014; 6(4):281–94. [PubMed: 24651194]
7. Chouinard CD, Wei MS, Beekman CR, Kemperman RHJ, Yost RA. Ion mobility in clinical analysis: current progress and future perspectives. Clin Chem. 2016; 62(1):124–33. [PubMed: 26585928]
8. May JC, Gant-Branum RL, McLean JA. Targeting the untargeted in molecular phenomics with structurally-selective ion mobility-mass spectrometry. Curr Opin Biotechnol. 2016; 39:192–97. [PubMed: 27132126]
9. Mason, E., McDaniel, E. Transport Properites of Ions in Gases. New York: Wiley; 1988.
10. Guevremont R, Siu KW, Wang J, Ding L. Combined ion mobility/time-of-flight mass spectrometry study of electrospray-generated ions. Anal Chem. 1997; 69(19):3959–65. [PubMed: 21639212]

11. Cohen MJ, Karasek FW. Plasma Chromatography™—a new dimension for gas chromatography and mass spectrometry. J Chromatogr Sci. 1970; 8(6):330–37.
12. Hoaglund CS, Valentine SJ, Sporleder CR, Reilly JP, Clemmer DE. Three-dimensional ion mobility/TOFMS analysis of electrosprayed biomolecules. Anal Chem. 1998; 70(11):2236–42. [PubMed: 9624897]
13. Wyttenbach T, Kemper PR, Bowers MT. Design of a new electrospray ion mobility mass spectrometer. Int J Mass Spectrom. 2001; 212(1–3):13–23.
14. Tang K, Shvartsburg AA, Lee HN, Prior DC, Buschbach MA, et al. High-sensitivity ion mobility spectrometry/mass spectrometry using electrodynamic ion funnel interfaces. Anal Chem. 2005; 77(10):3330–39. [PubMed: 15889926]
15. Pringle SD, Giles K, Wildgoose JL, Williams JP, Slade SE, et al. An investigation of the mobility separation of some peptide and protein ions using a new hybrid quadrupole/travelling wave IMS/oa-ToF instrument. Int J Mass Spectrom. 2007; 261(1):1–12.
16. Michelmann K, Silveira JA, Ridgeway ME, Park MA. Fundamentals of trapped ion mobility spectrometry. J Am Soc Mass Spectrom. 2015; 26(1):14–24. [PubMed: 25331153]
17. Ewing MA, Conant CRP, Zucker SM, Griffith KJ, Clemmer DE. Selected overtone mobility spectrometry. Anal Chem. 2015; 87(10):5132–38. [PubMed: 25892116]
18. Zucker SM, Ewing MA, Clemmer DE. Gridless overtone mobility spectrometry. Anal Chem. 2013; 85(21):10174–79. [PubMed: 24125033]
19. Rus J, Moro D, Sillero JA, Royuela J, Casado A, et al. IMS–MS studies based on coupling a differential mobility analyzer (DMA) to commercial API–MS systems. Int J Mass Spectrom. 2010; 298(1–3):30–40.
20. Brown LJ, Creaser CS. Field asymmetric waveform ion mobility spectrometry analysis of proteins and peptides: a review. Curr Anal Chem. 2013; 9(2):192–98.
21. Guevremont R. High-field asymmetric waveform ion mobility spectrometry: a new tool for mass spectrometry. J Chromatogr A. 2004; 1058(1–2):3–19. [PubMed: 15595648]
22. Kolakowski BM, Mester Z. Review of applications of high-field asymmetric waveform ion mobility spectrometry (FAIMS) and differential mobility spectrometry (DMS). Analyst. 2007; 132(9):842–64. [PubMed: 17710259]
23. Vidal-de-Miguel G, Macía M, Cuevas J. Transversal modulation ion mobility spectrometry (TM-IMS), a new mobility filter overcoming turbulence related limitations. Anal Chem. 2012; 84(18): 7831–37. [PubMed: 22924856]
24. May JC, McLean JA. Ion mobility-mass spectrometry: time-dispersive instrumentation. Anal Chem. 2015; 87(3):1422–36. [PubMed: 25526595]
25. Thomson JJ, Rutherford E. XL. On the passage of electricity through gases exposed to Röntgen rays. Phil Mag Ser 5. 1896; 42(258):392–407.
26. Von Helden G, Hsu MT, Kemper PR, Bowers MT. Structures of carbon cluster ions from 3 to 60 atoms: linears to rings to fullerenes. J Chem Phys. 1991; 95(5):3835–37.
27. Von Helden G, Hsu MT, Gotts N, Bowers MT. Carbon cluster cations with up to 84 atoms: structures, formation mechanism, and reactivity. J Phys Chem. 1993; 97(31):8182–92.
28. Shelimov KB, Hunter JM, Jarrold MF. Small carbon rings: dissociation, isomerization, and a simple-model based on strain. Int J Mass Spectrom. 1994; 138:17–31.
29. Hunter JM, Jarrold MF. Drift-tube studies of large carbon clusters: new isomers and the mechanism of giant fullerene formation. J Am Chem Soc. 1995; 117(41):10317–24.
30. Henderson SC, Valentine SJ, Counterman AE, Clemmer DE. ESI/ion trap/ion mobility/time-of-flight mass spectrometry for rapid and sensitive analysis of biomolecular mixtures. Anal Chem. 1999; 71(2):291–301. [PubMed: 9949724]
31. Hoaglund CS, Valentine SJ, Sporleder CR, Reilly JP, Clemmer DE. Three-dimensional ion mobility TOFMS analysis of electrosprayed biomolecules. Anal Chem. 1998; 70(11):2236–42. [PubMed: 9624897]
32. Bernstein SL, Dupuis NF, Lazo ND, Wyttenbach T, Condron MM, et al. Amyloid-β protein oligomerization and the importance of tetramers and dodecamers in the aetiology of Alzheimer's disease. Nat Chem. 2009; 1(4):326–31. [PubMed: 20703363]

33. Groessl M, Graf S, Knochenmuss R. High resolution ion mobility-mass spectrometry for separation and identification of isomeric lipids. Analyst. 2015; 140(20):6904–11. [PubMed: 26312258]
34. Liu YS, Valentine SJ, Counterman AE, Hoaglund CS, Clemmer DE. Injected-ion mobility analysis of biomolecules. Anal Chem. 1997; 69(23):A728–35.
35. Enders JR, McLean JA. Chiral and structural analysis of biomolecules using mass spectrometry and ion mobility-mass spectrometry. Chirality. 2009; 21(1e):E253–64. [PubMed: 19927374]
36. Belov ME, Buschbach MA, Prior DC, Tang K, Smith RD. Multiplexed ion mobility spectrometry-orthogonal time-of-flight mass spectrometry. Anal Chem. 2007; 79(6):2451–62. [PubMed: 17305309]
37. Clowers BH, Belov ME, Prior DC 3rd, Danielson WF, Ibrahim Y, Smith RD. Pseudorandom sequence modifications for ion mobility orthogonal time-of-flight mass spectrometry. Anal Chem. 2008; 80(7):2464–73. [PubMed: 18311942]
38. Kelly RT, Tolmachev AV, Page JS, Tang K, Smith RD. The ion funnel: theory, implementations, and applications. Mass Spectrom Rev. 2010; 29(2):294–312. [PubMed: 19391099]
39. Baker ES, Livesay EA, Orton DJ, Moore RJ, Danielson WF 3rd, et al. An LC-IMS-MS platform providing increased dynamic range for high-throughput proteomic studies. J Proteome Res. 2010; 9(2):997–1006. [PubMed: 20000344]
40. Kanu AB, Hill HH Jr. Ion mobility spectrometry detection for gas chromatography. J Chromatogr A. 2008; 1177(1):12–27. [PubMed: 18067900]
41. Creaser CS, Griffiths JR, Bramwell CJ, Noreen S, Hill CA, Thomas CLP. Ion mobility spectrometry: a review. Part 1 Structural analysis by mobility measurement. Analyst. 2004; 129(11):984–94.
42. Cook GW, LaPuma PT, Hook GL, Eckenrode BA. Using gas chromatography with ion mobility spectrometry to resolve explosive compounds in the presence of interferents. J Forensic Sci. 2010; 55(6):1582–91. [PubMed: 20735708]
43. Reyes-Garcés N, Gómez-Ríos GA, Souza Silva ÉA, Pawliszyn J. Coupling needle trap devices with gas chromatography–ion mobility spectrometry detection as a simple approach for on-site quantitative analysis. J Chromatogr A. 2013; 1300:193–98. [PubMed: 23768538]
44. Denawaka CJ, Fowlis IA, Dean JR. Evaluation and application of static headspace–multicapillary column-gas chromatography–ion mobility spectrometry for complex sample analysis. J Chromatogr A. 2014; 1338:136–48. [PubMed: 24630058]
45. Garrido-Delgado R, Dobao-Prieto MM, Arce L, Valcárcel M. Determination of volatile compounds by GC–IMS to assign the quality of virgin olive oil. Food Chem. 2015; 187:572–79. [PubMed: 25977065]
46. Wallace WT, Gazda DB, Limero TF, Minton JM, Macatangay AV, et al. Electrothermal vaporization sample introduction for spaceflight water quality monitoring via gas chromatography-differential mobility spectrometry. Anal Chem. 2015; 87(12):5981–88. [PubMed: 25971650]
47. Schumann A, Lenth C, Hasener J, Steckel V. Detection of volatile organic compounds from wood-based panels by gas chromatography-field asymmetric ion mobility spectrometry (GC-FAIMS). Int J Ion Mobil Spec. 2012; 15(3):157–68.
48. Crawford CL, Graf S, Gonin M, Fuhrer K, Zhang X, Hill HH. The novel use of gas chromatography-ion mobility-time of flight mass spectrometry with secondary electrospray ionization for complex mixture analysis. Int J Ion Mobil Spec. 2011; 14(1):23–30.
49. Klesper E, Corwin AH, Turner DA. High pressure gas chromatography above critical temperatures. J Org Chem. 1962; 27(2):700–6.
50. Taguchi K, Fukusaki E, Bamba T. Supercritical fluid chromatography/mass spectrometry in metabolite analysis. Bioanalysis. 2014; 6(12):1679–89. [PubMed: 25077627]
51. Desfontaine V, Guillarme D, Francotte E, Nováková L. Supercritical fluid chromatography in pharmaceutical analysis. J Pharm Biomed Anal. 2015; 113:56–71. [PubMed: 25818887]
52. Grand-Guillaume Perrenoud A, Guillarme D, Boccard J, Veuthey J-L, Barron D, Moco S. Ultra-high performance supercritical fluid chromatography coupled with quadrupole-time-of-flight mass spectrometry as a performing tool for bioactive analysis. J Chromatogr A. 2016; 1450:101–11. [PubMed: 27156735]

53. Rokushika S, Hatano H, Hill HH. Ion mobility spectrometry after supercritical fluid chromatography. Anal Chem. 1987; 59(1):8–12. [PubMed: 3826636]
54. Eatherton RL, Morrissey MA, Hill HH. Comparison of ion mobility constants of selected drugs after capillary gas chromatography and capillary supercritical fluid chromatography. Anal Chem. 1988; 60(20):2240–43. [PubMed: 3239796]
55. Wu C, Siems WF, Hill HH Jr, Hannan RM. Analytical determination of nicotine in tobacco by supercritical fluid chromatography–ion mobility detection. J Chromatogr A. 1998; 811(1–2):157–61.
56. Wu C, Siems WF, Hill HH, Hannan RM. Improved supercritical fluid chromatography–ion mobility spectrometry interface. J Microcolumn Sep. 1999; 11(4):251–57.
57. Beucher L, Dervilly-Pinel G, Cesbron N, Penot M, Gicquiau A, et al. Specific characterization of non-steroidal selective androgen peceptor modulators using supercritical fluid chromatography coupled to ion-mobility mass spectrometry: application to the detection of enobosarm in bovine urine. Drug Test Anal. 2016; 9(2):179–87. [PubMed: 26990774]
58. Sowell RA, Koeniger SL, Valentine SJ, Moon MH, Clemmer DE. Nanoflow LC/IMS-MS and LC/IMS-CID/MS of protein mixtures. J Am Soc Mass Spectrom. 2004; 15(9):1341–53. [PubMed: 15337515]
59. Crowell KL, Baker ES, Payne SH, Ibrahim YM, Monroe ME, et al. Increasing confidence of LC-MS identifications by utilizing ion mobility spectrometry. Int J Mass Spectrom. 2013; 354–55:312–17.
60. Valentine SJ, Kulchania M, Barnes CAS, Clemmer DE. Multidimensional separations of complex peptide mixtures: a combined high-performance liquid chromatography/ion mobility/time-of-flight mass spectrometry approach. Int J Mass Spectrom. 2001; 212(1–3):97–109.
61. Counterman AE, Hilderbrand AE, Barnes CAS, Clemmer DE. Formation of peptide aggregates during ESI: size, charge, composition, and contributions to noise. J Am Soc Mass Spectrom. 2001; 12(9):1020–35.
62. Valentine SJ, Plasencia MD, Liu XY, Krishnan M, Naylor S, et al. Toward plasma proteome profiling with ion mobility-mass spectrometry. J Proteome Res. 2006; 5(11):2977–84. [PubMed: 17081049]
63. Paglia G, Williams JP, Menikarachchi L, Thompson JW, Tyldesley-Worster R, et al. Ion mobility derived collision cross sections to support metabolomics applications. Anal Chem. 2014; 86(8):3985–93. [PubMed: 24640936]
64. Causon TJ, Hann S. Theoretical evaluation of peak capacity improvements by use of liquid chromatography combined with drift tube ion mobility-mass spectrometry. J Chromatogr A. 2015; 1416:47–56. [PubMed: 26372446]
65. Kyle JE, Zhang X, Weitz KK, Monroe ME, Ibrahim YM, et al. Uncovering biologically significant lipid isomers with liquid chromatography, ion mobility spectrometry and mass spectrometry. Analyst. 2016; 141(5):1649–59. [PubMed: 26734689]
66. Paglia G, Angel P, Williams JP, Richardson K, Olivos HJ, et al. Ion mobility-derived collision cross section as an additional measure for lipid fingerprinting and identification. Anal Chem. 2015; 87(2):1137–44. [PubMed: 25495617]
67. Sowell RA, Koeniger SL, Valentine SJ, Moon MH, Clemmer DE. Nanoflow LCAMS-MS and LCAMS-CID/MS of protein mixtures. J Am Soc Mass Spectrom. 2004; 15(9):1341–53. [PubMed: 15337515]
68. Liu XY, Valentine SJ, Plasencia MD, Trimpin S, Naylor S, Clemmer DE. Mapping the human plasma proteome by SCX-LC-IMS-MS. J Am Soc Mass Spectrom. 2007; 18(7):1249–64. [PubMed: 17553692]
69. Moon MH, Myung S, Plasencia M, Hilderbrand AE, Clemmer DE. Nanoflow LC/ion mobility/CID/TOF for proteomics: analysis of a human urinary proteome. J Proteome Res. 2003; 2(6):589–97. [PubMed: 14692452]
70. Baker ES, Burnum-Johnson KE, Ibrahim YM, Orton DJ, Monroe ME, et al. Enhancing bottom-up and top-down proteomic measurements with ion mobility separations. Proteomics. 2015; 15(16):2766–76. [PubMed: 26046661]

71. Baker ES, Burnum-Johnson KE, Jacobs JM, Diamond DL, Brown RN, et al. Advancing the high throughput identification of liver fibrosis protein signatures using multiplexed ion mobility spectrometry. Mol Cell Proteom. 2014; 13(4):1119–27.
72. Lareau NM, May JC, McLean JA. Non-derivatized glycan analysis by reverse phase liquid chromatography and ion mobility-mass spectrometry. Analyst. 2015; 140(10):3335–38. [PubMed: 25737268]
73. Liu X, Valentine SJ, Plasencia MD, Trimpin S, Naylor S, Clemmer DE. Mapping the human plasma proteome by SCX-LC-IMS-MS. J Am Soc Mass Spectrom. 2007; 18(7):1249–64. [PubMed: 17553692]
74. Stephan S, Hippler J, Köhler T, Deeb AA, Schmidt TC, Schmitz OJ. Contaminant screening of wastewater with HPLC-IM-qTOF-MS and LC+LC-IM-qTOF-MS using a CCS database. Anal Bioanal Chem. 2016; 408(24):6545–55. [PubMed: 27497965]
75. MacLean B, Tomazela DM, Shulman N, Chambers M, Finney GL, et al. Skyline: an open source document editor for creating and analyzing targeted proteomics experiments. Bioinformatics. 2010; 26(7):966–68. [PubMed: 20147306]
76. Sarafraz-Yazdi A, Amiri A. Liquid-phase microextraction. TRAC Trends Anal Chem. 2010; 29(1): 1–14.
77. Andrade-Eiroa A, Canle M, Leroy-Cancellieri V, Cerdà V. Solid-phase extraction of organic compounds: a critical review (Part I). TRAC Trends Anal Chem. 2016; 80:641–54.
78. Andrade-Eiroa A, Canle M, Leroy-Cancellieri V, Cerdà V. Solid-phase extraction of organic compounds: a critical review. Part II. TRAC Trends Anal Chem. 2016; 80:655–67.
79. Soulard P, McLaughlin M, Stevens J, Connolly B, Coli R, et al. Development of a high-throughput screening assay for stearoyl-CoA desaturase using rat liver microsomes, deuterium labeled stearoyl-CoA and mass spectrometry. Anal Chim Acta. 2008; 627(1):105–11. [PubMed: 18790133]
80. Lim KB, Özbal CC, Kassel DB. Development of a high-throughput online solid-phase extraction/ tandem mass spectrometry method for cytochrome P450 inhibition screening. J Biomol Screen. 2010; 15(4):447–52. [PubMed: 20208033]
81. Luippold AH, Arnhold T, Jörg W, Sussmuth RD. An integrated platform for fully automated high-throughput LC–MS/MS analysis of in vitro metabolic stability assay samples. Int J Mass Spectrom. 2010; 296(1–3):1–9.
82. Jian W, Romm MV, Edom RW, Miller VP, LaMarr WA, Weng N. Evaluation of a high-throughput online solid phase extraction–tandem mass spectrometry system for in vivo bioanalytical studies. Anal Chem. 2011; 83(21):8259–66. [PubMed: 21936562]
83. Hutchinson SE, Leveridge MV, Heathcote ML, Francis P, Williams L, et al. Enabling lead discovery for histone lysine demethylases by high-throughput RapidFire mass spectrometry. J Biomol Screen. 2012; 17(1):39–48. [PubMed: 21859681]
84. Razavi M, Frick LE, LaMarr WA, Pope ME, Miller CA, et al. High-throughput SISCAPA quantitation of peptides from human plasma digests by ultrafast, liquid chromatography-free mass spectrometry. J Proteome Res. 2012; 11(12):5642–49. [PubMed: 23126378]
85. Lowe DM, Gee M, Haslam C, Leavens B, Christodoulou E, et al. Lead discovery for human kynurenine 3-monooxygenase by high-throughput RapidFire mass spectrometry. J Biomol Screen. 2014; 19(4):508–15. [PubMed: 24381207]
86. Rye PT, LaMarr WA. Measurement of glycolysis reactants by high-throughput solid phase extraction with tandem mass spectrometry: characterization of pyrophosphate-dependent phosphofructokinase as a case study. Anal Biochem. 2015; 482:40–47. [PubMed: 25849585]
87. Zhang X, Romm M, Zheng X, Zink EM, Kim Y-M, et al. SPE-IMS-MS: an automated platform for sub-sixty second surveillance of endogenous metabolites and xenobiotics in biofluids. Clin Mass Spectrom. 2016 In press.
88. Arthur CL, Pawliszyn J. Solid phase microextraction with thermal desorption using fused silica optical fibers. Anal Chem. 1990; 62(19):2145–48.
89. Vas G, Vékey K. Solid-phase microextraction: a powerful sample preparation tool prior to mass spectrometric analysis. J Mass Spectrom. 2004; 39(3):233–54. [PubMed: 15039931]

90. Li X, Zeng Z, Zeng Y. Solid-phase microextraction coupled to gas chromatography for the determination of 2,3-dimethyl-2,3-dinitrobutane as a marking agent for explosives. Talanta. 2007; 72(4):1581–85. [PubMed: 19071800]
91. Alvarez-Rivera G, Vila M, Lores M, Garcia-Jares C, Llompart M. Development of a multi-preservative method based on solid-phase microextraction–gas chromatography–tandem mass spectrometry for cosmetic analysis. J Chromatogr A. 2014; 1339:13–25. [PubMed: 24661872]
92. Pereira J, Silva CL, Perestrelo R, Gonçalves J, Alves V, Câmara JS. Re-exploring the high-throughput potential of microextraction techniques, SPME and MEPS, as powerful strategies for medical diagnostic purposes. Innovative approaches, recent applications and future trends. Anal Bioanal Chem. 2014; 406(8):2101–22. [PubMed: 24442008]
93. Rearden P, Harrington PB. Rapid screening of precursor and degradation products of chemical warfare agents in soil by solid-phase microextraction ion mobility spectrometry (SPME–IMS). Anal Chim Acta. 2005; 545(1):13–20.
94. Wang Y, Nacson S, Pawliszyn J. The coupling of solid-phase microextraction/surface enhanced laser desorption/ionization to ion mobility spectrometry for drug analysis. Anal Chim Acta. 2007; 582(1):50–54. [PubMed: 17386473]
95. Lai H, Leung A, Magee M, Almirall JR. Identification of volatile chemical signatures from plastic explosives by SPME-GC/MS and detection by ion mobility spectrometry. Anal Bioanal Chem. 2010; 396(8):2997–3007. [PubMed: 20229010]
96. Holopainen S, Luukkonen V, Nousiainen M, Sillanpää M. Determination of chlorophenols in water by headspace solid phase microextraction ion mobility spectrometry (HS-SPME-IMS). Talanta. 2013; 114:176–82. [PubMed: 23953458]
97. Jafari MT, Saraji M, Ameri AH. Coupling of solid phase microextraction with electrospray ionization ion mobility spectrometry and direct analysis of venlafaxine in human urine and plasma. Anal Chim Acta. 2015; 853:460–68. [PubMed: 25467491]
98. Revercomb HE, Mason EA. Theory of plasma chromatography gaseous electrophoresis—a review. Anal Chem. 1975; 47(7):970–83.
99. Giddings JC. Generation of variance, “theoretical plates,” resolution, and peak capacity in electrophoresis and sedimentation. Sep Sci Tech. 1969; 4(3):181–89.
100. Hjerten S. Free zone electrophoresis—preliminary note. Ark Kemi. 1958; 13(1–2):151–52.
101. Hjerten S, Zhu MD. Micropreparative version of high-performance electrophoresis: the electrophoretic counterpart of narrow-bore high-performance liquid-chromatography. J Chromatogr. 1985; 327:157–64.
102. Jorgenson JW, Lukacs KD. Free-zone electrophoresis in glass-capillaries. Clin Chem. 1981; 27(9):1551–53. [PubMed: 7261333]
103. Moore AW, Jorgenson JW. Rapid comprehensive 2-dimensional separations of peptides via RPLC optically gated capillary zone electrophoresis. Anal Chem. 1995; 67(19):3448–55. [PubMed: 8686893]
104. Leriche ED, Afonso C, Lange CM, Grossel MC, Truong L, et al. Glycine-modified polyamidoamine dendrimers: synthesis and structural characterization using nuclear magnetic resonance, ion-mobility mass spectrometry and capillary electrophoresis. RSC Adv. 2014; 4(4): 1744–53.
105. Mironov GG, Okhonin V, Khan N, Clouthier CM, Berezovski MV. Conformational dynamics of DNA G-quadruplex in solution studied by kinetic capillary electrophoresis coupled on-line with mass spectrometry. ChemistryOpen. 2014; 3(2):58–64. [PubMed: 24808992]
106. Hallen RW, Shumate CB, Siems WF, Tsuda T, Hill HH. Preliminary investigation of ion mobility spectrometry after capillary electrophoretic introduction. J Chromatogr. 1989; 480:233–45. [PubMed: 2592482]
107. Shumate CB, Hill HH. Coronaspray nebulization and ionization of liquid samples for ion mobility spectrometry. Anal Chem. 1989; 61(6):601–6. [PubMed: 2729593]
108. Li J, Purves RW, Richards JC. Coupling capillary electrophoresis and high-field asymmetric waveform ion mobility spectrometry mass spectrometry for the analysis of complex lipopolysaccharides. Anal Chem. 2004; 76(16):4676–83. [PubMed: 15307776]

109. Venne K, Bonneil E, Eng K, Thibault P. Improvement in peptide detection for proteomics analyses using nanoLC-MS and high-field asymmetry waveform ion mobility mass spectrometry. Anal Chem. 2005; 77(7):2176–86. [PubMed: 15801752]
110. Moini M. Capillary electrophoresis mass spectrometry and its application to the analysis of biological mixtures. Anal Bioanal Chem. 2002; 373(6):466–80. [PubMed: 12172682]
111. Guo XJ, Fillmore TL, Gao YQ, Tang KQ. Capillary electrophoresis-nanoelectrospray ionization-selected reaction monitoring mass spectrometry via a true sheathless metal-coated emitter interface for robust and high-sensitivity sample quantification. Anal Chem. 2016; 88(8):4418–25. [PubMed: 27028594]
112. Maxwell EJ, Zhong XF, Zhang H, van Zeijl N, Chen DDY. Decoupling CE and ESI for a more robust interface with MS. Electrophoresis. 2010; 31(7):1130–37. [PubMed: 20196027]
113. Sun LL, Zhu GJ, Zhang ZB, Mou S, Dovichi NJ. Third-generation electrokinetically pumped sheath-flow nanospray interface with improved stability and sensitivity for automated capillary zone electrophoresis-mass spectrometry analysis of complex proteome digests. J Proteome Res. 2015; 14(5):2312–21. [PubMed: 25786131]
114. Wojcik R, Dada OO, Sadilek M, Dovichi NJ. Simplified capillary electrophoresis nanospray sheath-flow interface for high efficiency and sensitive peptide analysis. Rapid Commun Mass Spectrom. 2010; 24(17):2554–60. [PubMed: 20740530]
115. Gorshkov M. USSR inventor's certificate no. 966583. Byull Izobret. 1982; (38)
116. Guevremont R. High-field asymmetric waveform ion mobility spectrometry: a new tool for mass spectrometry. J Chromatogr A. 2004; 1058(1):3–19. [PubMed: 15595648]
117. Shvartsburg AA, Tang K, Smith RD. Optimization of the design and operation of FAIMS analyzers. J Am Soc Mass Spectrom. 2005; 16(1):2–12. [PubMed: 15653358]
118. Viehland LA, Guevremontb R, Purves RW, Barnett DA. Comparison of high-field ion mobility obtained from drift tubes and a FAIMS apparatus. Int J Mass Spectrom. 2000; 197(1):123–30.
119. Hatsis P, Kapron JT. A review on the application of high-field asymmetric waveform ion mobility spectrometry (FAIMS) in drug discovery. Rapid Commun Mass Spectrom. 2008; 22(5):735–38. [PubMed: 18257113]
120. Brown LJ, Toutoungi DE, Devenport NA, Reynolds JC, Kaur-Atwal G, et al. Miniaturized ultra high field asymmetric waveform ion mobility spectrometry combined with mass spectrometry for peptide analysis. Anal Chem. 2010; (82):9827–34. [PubMed: 21049936]
121. De La Mora JF, Ude S, Thomson BA. The potential of differential mobility analysis coupled to MS for the study of very large singly and multiply charged proteins and protein complexes in the gas phase. Biotechnol J. 2006; 1(9):988–97. [PubMed: 16941442]
122. Shvartsburg AA, Tang K, Smith RD, Holden M, Rush M, et al. Ultrafast differential ion mobility spectrometry at extreme electric fields coupled to mass spectrometry. Anal Chem. 2009; 81(19): 8048–53. [PubMed: 19708673]
123. Xuan Y, Creese AJ, Horner JA, Cooper HJ. High-field asymmetric waveform ion mobility spectrometry (FAIMS) coupled with high-resolution electron transfer dissociation mass spectrometry for the analysis of isobaric phosphopeptides. Rapid Commun Mass Spectrom. 2009; 23(13):1963–69. [PubMed: 19504484]
124. Kaszycki JL, Bowman AP, Shvartsburg AA. Ion mobility separation of peptide isotopomers. J Am Soc Mass Spectrom. 2016; 27(5):795–99. [PubMed: 26944281]
125. Papadopoulos G, Svendsen A, Boyarkin OV, Rizzo TR. Conformational distribution of bradykinin $[bk + 2\ H]^{2+}$ revealed by cold ion spectroscopy coupled with FAIMS. J Am Soc Mass Spectrom. 2012; 23(7):1173–81. [PubMed: 22528205]
126. Bohrer BC, Merenbloom SI, Koeniger SL, Hilderbrand AE, Clemmer DE. Biomolecule analysis by ion mobility spectrometry. Annu Rev Anal Chem. 2008; 1:293–327.
127. Saba J, Bonneil E, Pomies C, Eng K, Thibault P. Enhanced sensitivity in proteomics experiments using FAIMS coupled with a hybrid linear ion trap/orbitrap mass spectrometer. J Proteome Res. 2009; 8(7):3355–66. [PubMed: 19469569]
128. McLean JA, Ruotolo BT, Gillig KJ, Russell DH. Ion mobility–mass spectrometry: a new paradigm for proteomics. Int J Mass Spectrom. 2005; 240(3):301–15.

129. Bonneil E, Pfammatter S, Thibault P. Enhancement of mass spectrometry performance for proteomic analyses using high-field asymmetric waveform ion mobility spectrometry (FAIMS). J Mass Spectrom. 2015; 50(11):1181–95. [PubMed: 26505763]
130. Kliman M, May JC, McLean JA. Lipid analysis and lipidomics by structurally selective ion mobility-mass spectrometry. Biochim Biophys Acta Mol Cell Biol Lipids. 2011; 1811(11):935–45.
131. Jackson SN, Ugarov M, Egan T, Post JD, Langlais D, et al. MALDI-ion mobility-TOFMS imaging of lipids in rat brain tissue. J Mass Spectrom. 2007; 42(8):1093–98. [PubMed: 17621389]
132. Fenn LS, Kliman M, Mahsut A, Zhao SR, McLean JA. Characterizing ion mobility-mass spectrometry conformation space for the analysis of complex biological samples. Anal Bioanal Chem. 2009; 394(1):235–44. [PubMed: 19247641]
133. Tang K, Li F, Shvartsburg AA, Strittmatter EF, Smith RD. Two-dimensional gas-phase separations coupled to mass spectrometry for analysis of complex mixtures. Anal Chem. 2005; 77(19):6381–88. [PubMed: 16194103]
134. Wilks A, Hart M, Koehl A, Somerville J, Boyle B, Ruiz-Alonso D. Characterization of a miniature, ultra-high-field, ion mobility spectrometer. Int J Ion Mobil Spec. 2012; 15(3):199–222.
135. Schneider BB, Covey TR, Coy SL, Krylov EV, Nazarov EG. Planar differential mobility spectrometer as a pre-filter for atmospheric pressure ionization mass spectrometry. Int J Mass Spectrom. 2010; 298(1–3):45–54. [PubMed: 21278836]
136. Zhang X, Ibrahim YM, Chen T-C, Kyle JE, Norheim RV, et al. Enhancing biological analyses with three dimensional field asymmetric ion mobility, low field drift tube ion mobility and mass spectrometry (μFAIMS/IMS-MS) separations. Analyst. 2015; 140(20):6955–63. [PubMed: 26140287]
137. Sackmann EK, Fulton AL, Beebe DJ. The present and future role of microfluidics in biomedical research. Nature. 2014; 507:181–89. [PubMed: 24622198]
138. Volpatti LR, Yetisen AK. Commercialization of microfluidic devices. Trends Biotechnol. 2014; 32(7):347–50. [PubMed: 24954000]
139. Gao D, Liu H, Jiang Y, Lin J-M. Recent advances in microfluidics combined with mass spectrometry: technologies and applications. Lab Chip. 2013; 13(17):3309–22. [PubMed: 23824006]
140. Feng X, Liu B-F, Li J, Liu X. Advances in coupling microfluidic chips to mass spectrometry. Mass Spectrom Rev. 2015; 34(5):535–57. [PubMed: 24399782]
141. Wang X, Yi L, Mukhitov N, Schrell AM, Dhumpa R, Roper MG. Microfluidics-to-mass spectrometry: a review of coupling methods and applications. J Chromatogr A. 2015; 1382:98–116. [PubMed: 25458901]
142. Cong Y, Katipamula S, Trader CD, Orton DJ, Geng T, et al. Mass spectrometry-based monitoring of millisecond protein-ligand binding dynamics using an automated microfluidic platform. Lab Chip. 2016; 16(9):1544–48. [PubMed: 27009517]
143. Enders JR, Marasco CC, Kole A, Nguyen B, Sevugarajan S, et al. Towards monitoring real-time cellular response using an integrated microfluidicsmatrix assisted laser desorption ionisation/nanoelectrospray ionisation-ion mobility-mass spectrometry platform. IET Syst Biol. 2010; 4(6):416–27. [PubMed: 21073240]
144. Marasco CC, Enders JR, Seale KT, McLean JA, Wikswo JP. Real-time cellular exometabolome analysis with a microfluidic-mass spectrometry platform. PLOS ONE. 2015; 10(2):e0117685. [PubMed: 25723555]
145. Revercomb HE, Mason EA. Theory of plasma chromatography/gaseous electrophoresis—a review. Anal Chem. 1975; 47(7):970–83.
146. Merenbloom SI, Glaskin RS, Henson ZB, Clemmer DE. High-resolution ion cyclotron mobility spectrometry. Anal Chem. 2009; 81(4):1482–87. [PubMed: 19143495]
147. Kemper PR, Dupuis NF, Bowers MT. A new, higher resolution, ion mobility mass spectrometer. Int J Mass Spectrom. 2009; 287(1–3):46–57.

148. Giles, K.Wildgoose, JL.Pringle, S.Langridge, D.Nixon, P., et al., editors. Characterising a T-wave enabled multi-pass cyclic ion mobility separator; Presented at Am. Soc. Mass. Spectrom. Conf., 63rd; St. Louis, MO. 2015.

149. Deng L, Ibrahim YM, Baker ES, Aly NA, Hamid AM, et al. Ion mobility separations of isomers based upon long path length structures for lossless ion manipulations combined with mass spectrometry. Chem Select. 2016; 1(10):2396–99.

150. Deng L, Ibrahim YM, Hamid AM, Garimella SVB, Webb IK, et al. Ultra-high resolution ion mobility separations utilizing traveling waves in a 13-m serpentine path length structures for lossless ion manipulations module. Anal Chem. 2016; 88(18):8957–64. [PubMed: 27531027]

151. Garimella SVB, Ibrahim YM, Tang K, Webb IK, Baker ES, et al. Spatial ion peak compression and its utility in ion mobility spectrometry. J Am Soc Mass Spectrom. 2016; 27(6):1–8. [PubMed: 27126468]

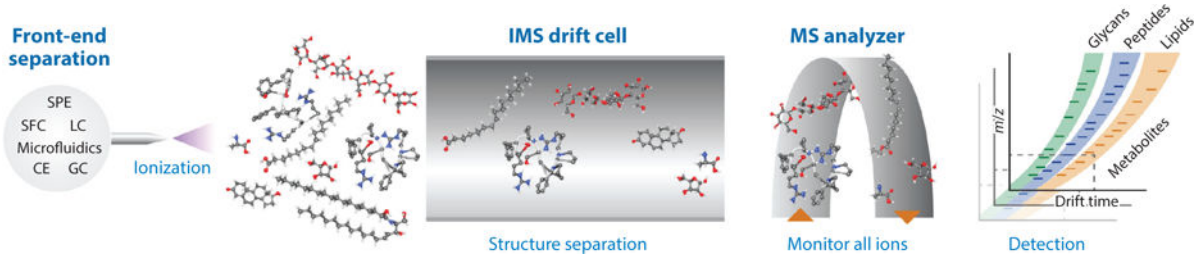

Figure 1.

A schematic showing three-dimensional analyses, where different front-end separation techniques are performed prior to the IMS separation and MS detection. This enhances multi-omic analyses of complex biological and environmental samples. Abbreviations: CE, capillary electrophoresis; GC, gas chromatography; IMS, ion mobility spectrometry; LC, liquid chromatography; MS, mass spectrometry; SFC, supercritical fluid chromatography; SPE, solid-phase extraction.

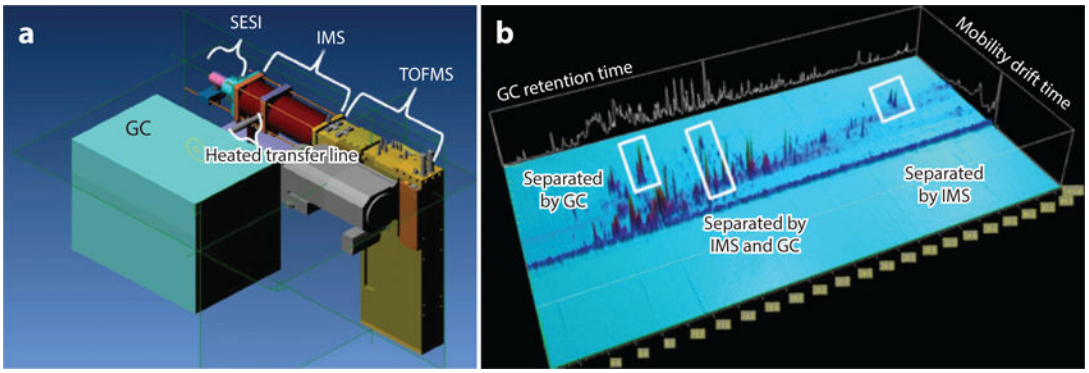

Figure 2.

(*a*) A diagram of the instrumental setup for the GC-DTIMS-MS experiments and (*b*) the spectra for lavender oil illustrated with GC retention time (in minutes), DTIMS drift time (in milliseconds), and total ion intensity (in arbitrary units). The peaks highlighted in white boxes were only separated by the dimensions defined in the figure. Reproduced with permission from Reference 48. Copyright 2010, Springer. Abbreviations: DTIMS, drift tube IMS; GC, gas chromatography; IMS, ion mobility spectrometry; MS, mass spectrometry; SESI, secondary electrospray ionization; TOFMS, time-of-flight MS.

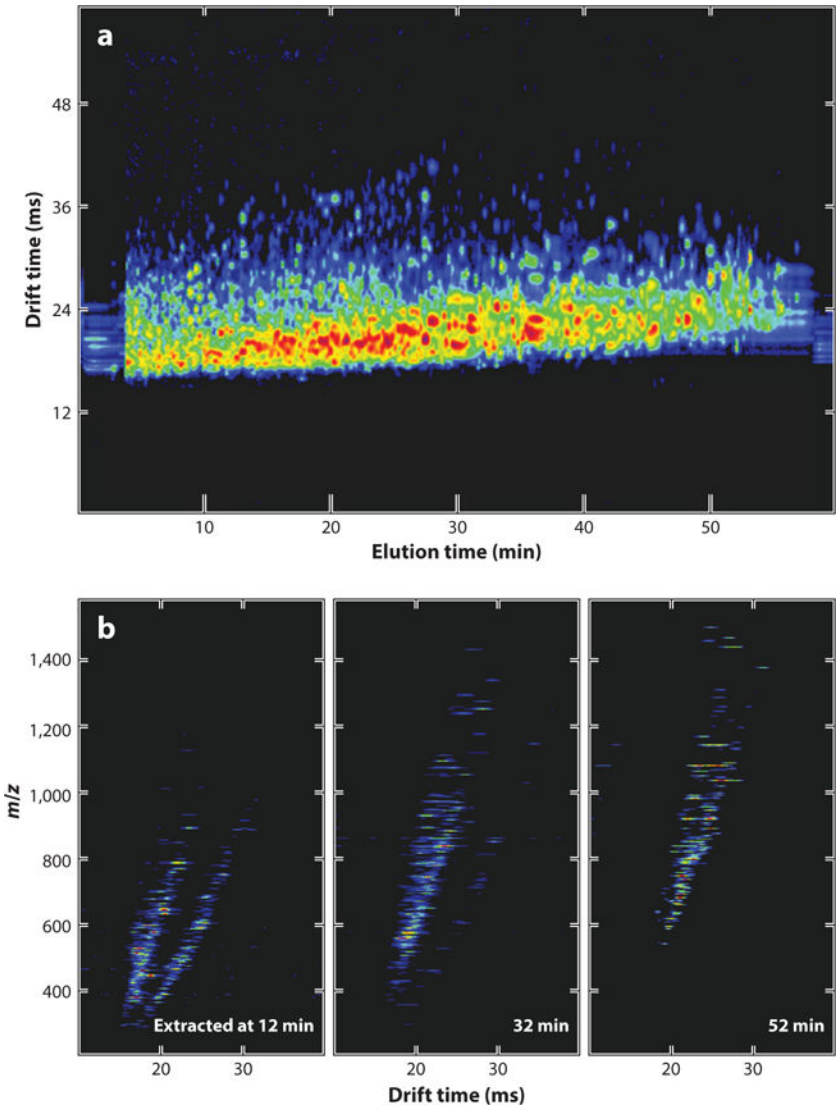

Figure 3.

(*a*) The 1-h LC-DTIMS-MS separation of human serum shown as a function of LC elution and DTIMS drift time. (*b*) Three different 1-s DTIMS-MS spectra extracted from those in panel *a* at 12, 32, and 52 min to exemplify the many different peptides detected as a function of LC elution time, DTIMS drift time, and *m*/*z* ratios. Reproduced with permission from Reference 59. Copyright 2013, Elsevier. Abbreviations: DTIMS, drift tube ion mobility spectrometry; LC, liquid chromatography; MS, mass spectrometry.

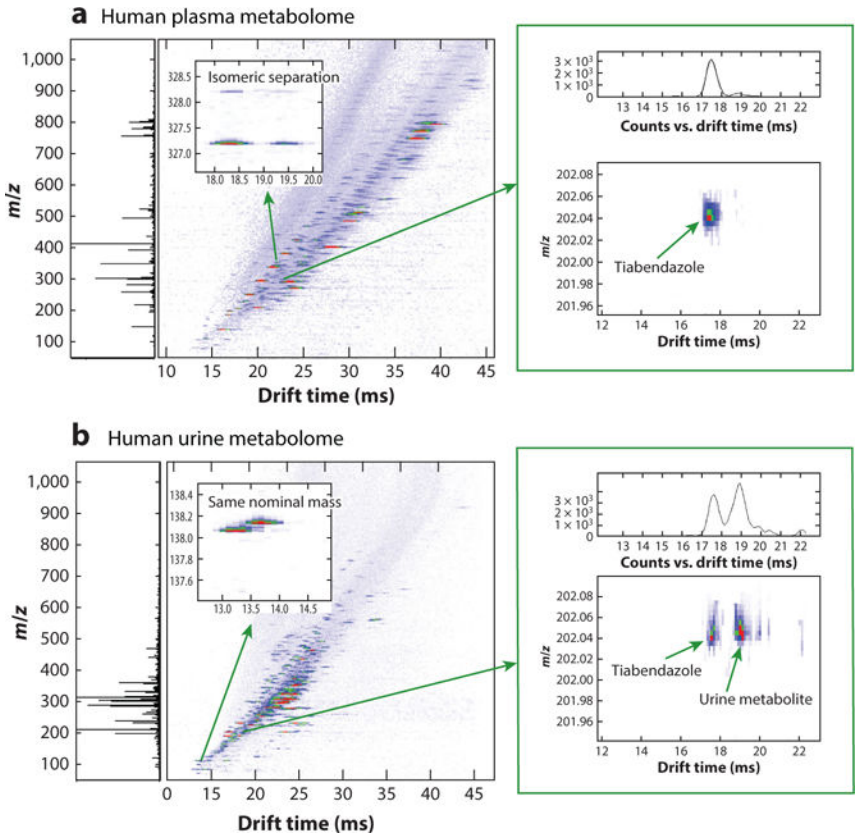

Figure 4.

The 5-s SPE-DTIMS-MS analyses of (*a*) human plasma and (*b*) urine extracts with the spiked xenobiotics, including 1 nM of tiabendazole. Thousands of small molecule features were detected simultaneously in the discovery analyses, and isomeric features were well separated, as shown in panel *a*, for m/z = 327.197. Features with the same nominal mass were also distinguished by DTIMS (m/z = 138.054 and 138.129), as shown in panel *b*, which is very important for preselection prior to MS/MS analyses with wide selection windows. Additionally, the 1-nM concentration of tiabendazole was detected in both human plasma and urine extracts with similar signal intensities, indicating no matrix effects for the different biofluids. Reproduced with permission from Reference 87. Copyright 2016, Elsevier. Abbreviations: IMS, ion mobility spectrometry; MS, mass spectrometry; SPE, solid-phase extraction.

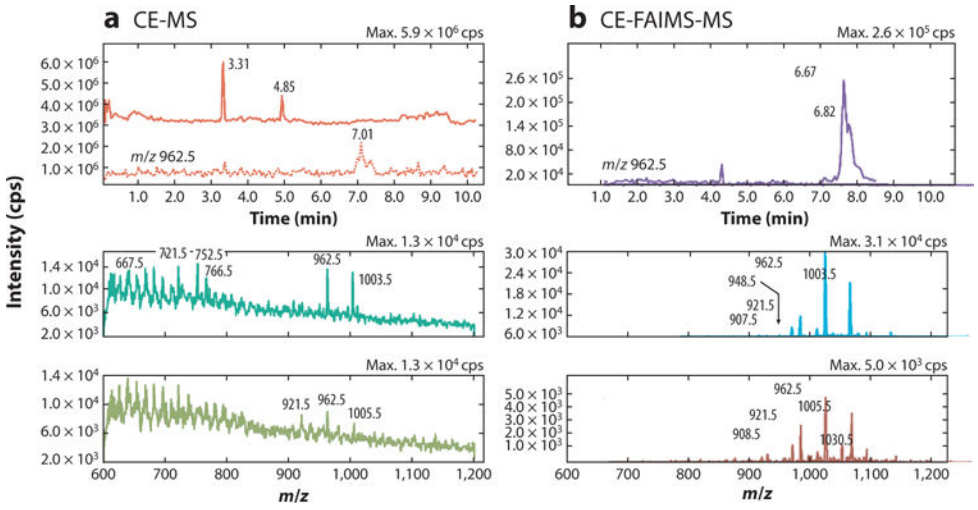

Figure 5.

(*a*) CE-MS and (*b*) CE-FAIMS-MS spectra of 1 ng/μL of O-deacylated LPS from *Haemophilus influenzae* strain 375. The top panels show the total ion extraction for *m*/*z* 600–1,200, with the extracted ion chromatogram for *m*/*z* 962.5 also shown for CE-MS. The middle panels show the extracted mass spectra for 6.5 to 7.1 min. The bottom panels illustrate the extracted mass spectra for 6.8 to 7.1 min. Reproduced with permission from Reference 108. Copyright 2004, American Chemical Society. Abbreviations: CE, capillary electrophoresis; cps, counts per second; FAIMS, field asymmetric ion mobility spectrometry; LPS, lipopolysasscharides; MS, mass spectrometry.

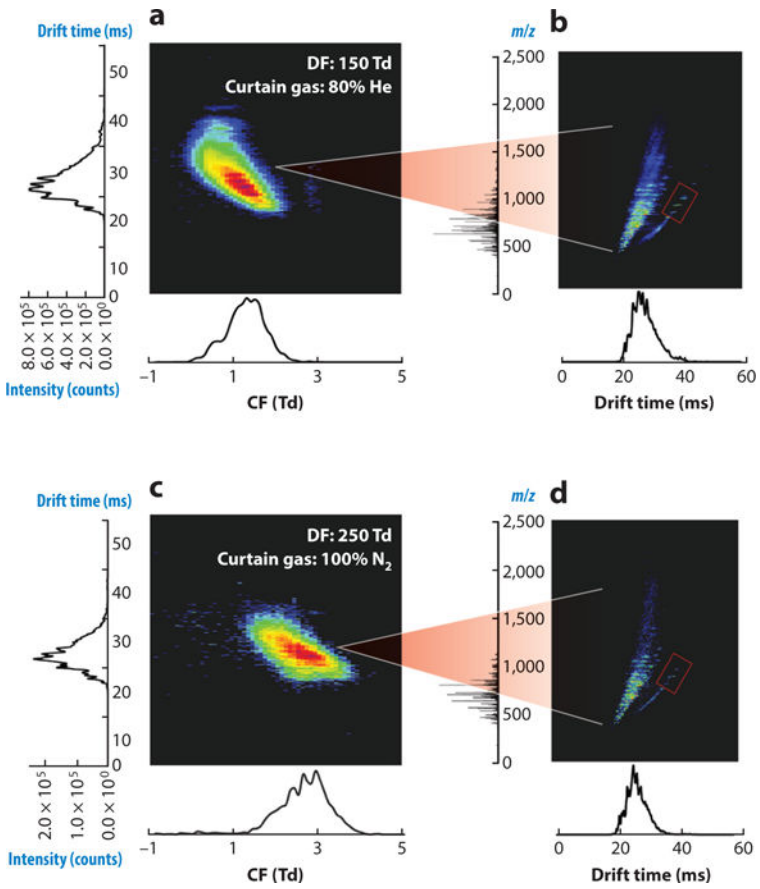

Figure 6.

The μFAIMS-DTIMS-MS three-dimensional separations of bovine serum albumin tryptic digest at (*a*) a DF of 150 Td with He/N_2 and (*c*) a DF of 250 Td with N_2 as curtain gases. The *x* dimension represents the CF FAIMS dimension, and the *y* axis shows the DTIMS dimension. To further illustrate the DTIMS-MS two-dimensional spectra, panels *b* and *d* are extracted with DTIMS on the *x* axis and with MS on the *y* axis. The red boxes in panels *b* and *d* illustrate the feature sensitivity differences between the two gas compositions. Reproduced with permission from Reference 136. Copyright 2015, Royal Society of Chemistry. Abbreviations: CF, compensation field; DF, dispersion field; DTIMS, drift tube IMS; FAIMS, field asymmetric IMS; He, helium; IMS, ion mobility spectrometry; MS, mass spectrometry; N_2, nitrogen; Td, Townsend.

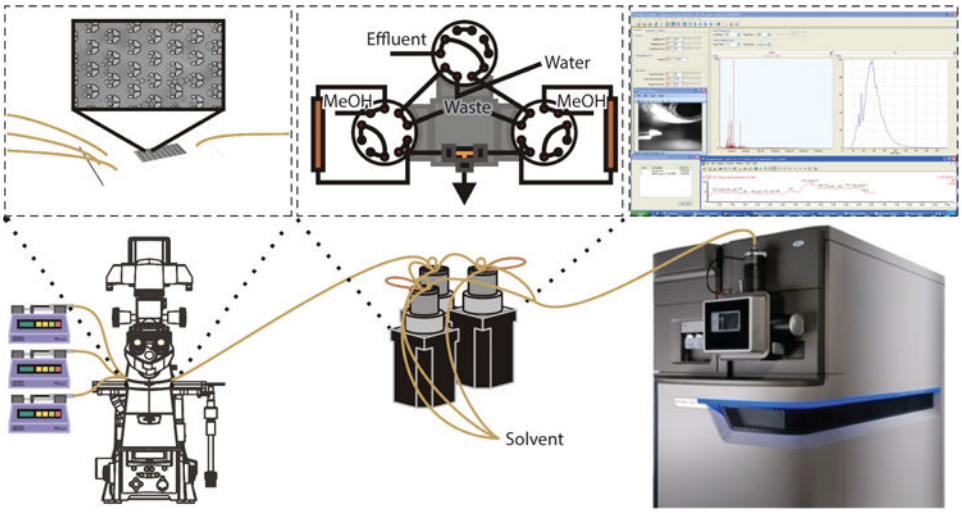

Figure 7.

A microfluidic-TWIMS-MS platform utilizing an MTNP-SPE-nanoESI-IMS-MS platform for the real-time analysis of cellular response to drugs and perturbations. Reproduced with permission from Reference 144 under the terms of the Creative Commons Attribution 4.0 International License, http://creativecommons.org/licenses/by/4.0. Abbreviations: ESI, electrospray ionization; IMS, ion mobility spectrometry; MeOH, methanol; MS, mass spectrometry; MTNP, multitrap nanophysiometer; SPE, solid-phase extraction; TWIMS, traveling wave IMS.

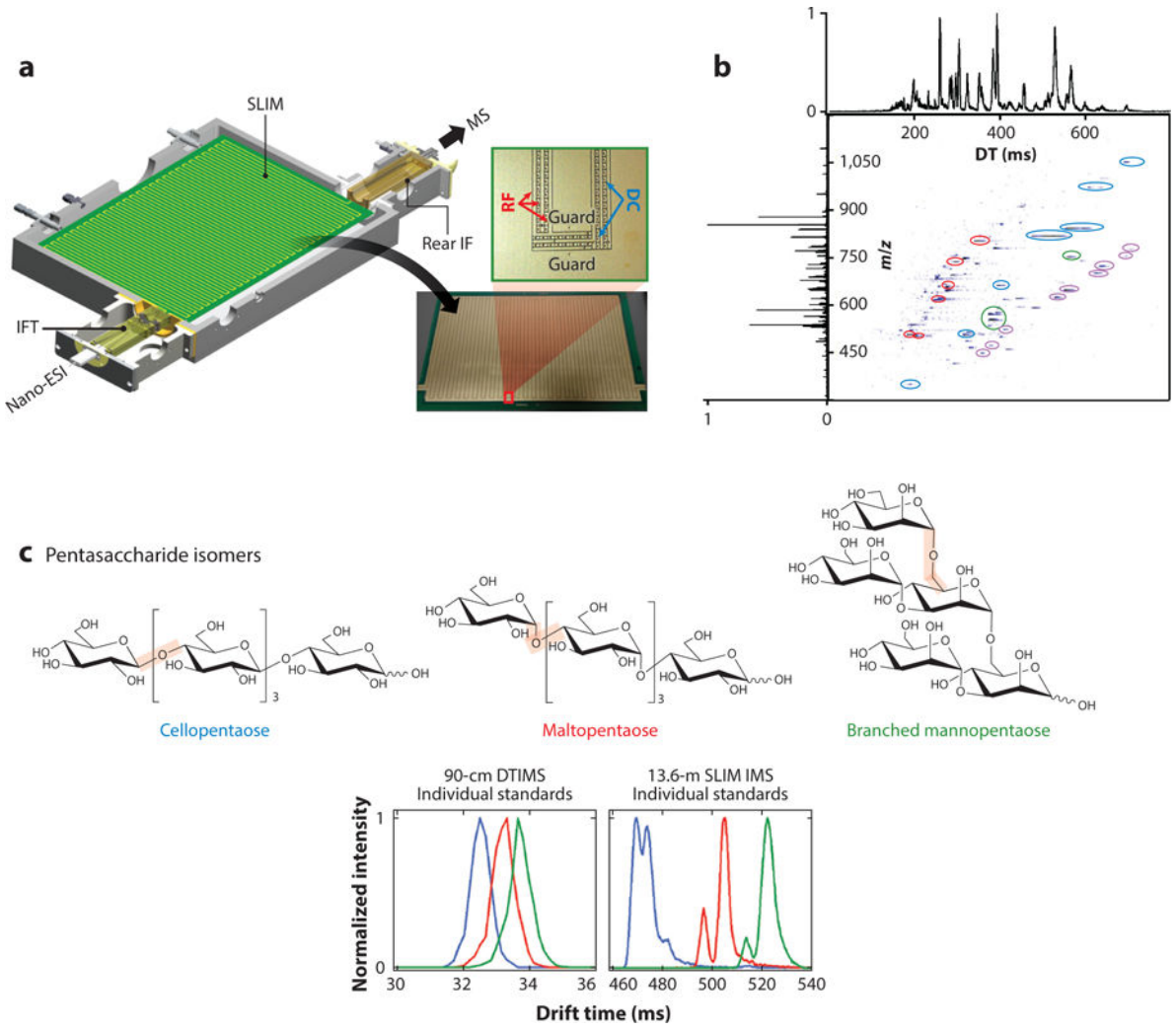

Figure 8.

(*a*) A schematic and photograph of the serpentine 13-m SLIM IMS-MS platform. (*b*) The two-dimensional nested IMS-MS spectrum from the SLIM platform showing DT versus *m*/*z* for the peptide/carbohydrate/lipid mixture analyzed. Different molecular classes typically separate by different trend lines due to the distinct backbone structures of each molecule type, with the 2+ peptides arriving first (*red*), followed by 1+ glycans (*blue*), 1+ peptides (*green*), and finally the 1+ lipids (*pink*). (*c*) Comparison of IMS separations of isomeric oligosaccharides by the 90-cm DTIMS and 13-m SLIM IMS. Reproduced with permission from Reference 149. Copyright 2016, John Wiley & Sons. Abbreviations: DC, direct current; DT, drift time; DTIMS, drift tube IMS; ESI, electrospray ionization; IF, ion funnel; IFT, ion funnel trap; IMS, ion mobility spectrometry; MS, mass spectrometry; RF, radio frequency; SLIM, structure for lossless ion manipulations.

Table 1

Advantages and disadvantages of different front-end separation techniques

Technique	Analysis time	Advantages	Disadvantages
GC	Minutes to hours	Allows high peak capacity small-molecule analyses; chromatography is highly reproducible	Is limited to volatile compounds; high temperature can induce decomposition
SFC	Minutes	Provides fast separations; is orthogonal to reverse-phase LC	Works best for nonpolar molecules
LC	Minutes to hours	Is applicable to many molecule types; allows high peak capacity small-molecule analyses	Has limited throughput because long separation times provide the best measurements
SPE	Seconds to minutes	Provides ultrafast separations; is ideal for sample desalting and molecular class extraction	Has low or no peak capacity, so it is similar to direct infusion
CE	Minutes	Has low sample consumption	Lacks orthogonality with DTIMS
FAIMS	Milliseconds to seconds	Allows high-throughput analyses; reduces noise and interferences	Experiences large ion losses due to its scanning characteristics; separation occurs after ionization, which does not help ionization suppression problems
Microfluidics	Seconds to hours	Is automatable; allows high-throughput analyses; requires minimal sample	Loading large amounts of samples is difficult, resulting in lower sensitivity for abundant samples

Abbreviations: CE, capillary electrophoresis; DTIMS, drift tube IMS; FAIMS, field asymmetric IMS; GC, gas chromatography; IMS, ion mobility spectrometry; LC, liquid chromatography; SFC, supercritical fluid chromatography; SPE, solid-phase extraction.